

HUBBLE SPACE TELESCOPE OBSERVATIONS OF THE DRACO DWARF SPHEROIDAL GALAXY¹

CARL J. GRILLMAIR,² JEREMY R. MOULD,³ JON A. HOLTZMAN,⁴ GUY WORTHEY,^{5,6} GILDA E. BALLESTER,⁷
CHRISTOPHER J. BURROWS,⁸ JOHN T. CLARKE,⁷ DAVID CRISP,⁹ ROBIN W. EVANS,⁹
JOHN S. GALLAGHER III,¹⁰ RICHARD E. GRIFFITHS,¹¹ J. JEFF HESTER,¹²
JOHN G. HOESSEL,¹⁰ PAUL A. SCOWEN,¹² KARL R. STAPELFELDT,⁹
JOHN T. TRAUGER,⁹ ALAN M. WATSON,⁴
AND JAMES A. WESTPHAL¹³

Received 1997 June 18; revised 1997 September 24

ABSTRACT

We present an F606W–F814W color-magnitude diagram for the Draco dwarf spheroidal galaxy based on *Hubble Space Telescope* Wide Field Planetary Camera 2 (WFPC2) images. The luminosity function is well sampled to ~ 3 mag below the turnoff. We see no evidence for multiple turnoffs and conclude that, at least over the field of view of the WFPC2, star formation was primarily single-epoch. If the observed number of blue stragglers is due to extended star formation, then roughly 6% (upper limit) of the stars could be half as old as the bulk of the galaxy. The color difference between the red giant branch and the turnoff is consistent with an old population and is very similar to that observed in the old, metal-poor Galactic globular clusters M68 and M92. Despite its red horizontal branch, Draco appears to be older than M68 and M92 by 1.6 ± 2.5 Gyr, lending support to the argument that the “second parameter” that governs horizontal-branch morphology must be something other than age. Draco’s observed luminosity function is very similar to that of M68, and the derived initial mass function is consistent with that of the solar neighborhood.

Key words: galaxies: abundances — galaxies: elliptical and lenticular, cD — galaxies: evolution — galaxies: individual (Draco) — Local Group

1. INTRODUCTION

Galaxies like the Draco dwarf spheroidal system may be the building blocks of the universe (Koo et al. 1994). Draco is among the faintest known galaxies and, indeed, at $2 \times 10^5 L_{\odot}$, ranks among the middling globular clusters in luminosity. However, its very extended distribution of stars ($D \sim 0.5$ kpc) clearly distinguishes it from the comparatively tightly condensed globulars. Moreover, the assumption of dynamical equilibrium leads one to very high estimates for

the mass-to-light ratio (Aaronson 1983), with recent multi-fiber spectroscopy yielding a remarkable $M/L = 90 \pm 15$ (Armandroff, Olszewski, & Pryor 1995). If the dark matter is primarily stellar, as might be inferred from the findings of recent microlensing experiments, then the initial mass function (IMF) in these galaxies might have been very different from the present-day IMF in our own Galaxy. It is clearly important to try to piece together the star formation histories of such galaxies, as this may have important consequences for ideas concerning the formation and evolution of more luminous galaxies like our own.

The color-magnitude diagram (CMD) of the Draco dwarf was first studied by Baade & Swope (1961) and found to be generally similar to the CMDs of metal-poor globular clusters, with the exception that it has a rather broad giant branch. Baade & Swope also first detected the “anomalous” Cepheids, more luminous than the period-luminosity relation for type II Cepheids would predict, and now known to be characteristic of dwarf galaxies. Another marked anomaly in the CMD is Draco’s red horizontal branch, which is incompatible with low metallicity in a Population II system (the second-parameter problem). This phenomenon alone could be taken to suggest that Draco is $\sim 2 \times 10^9$ yr younger than classic, metal-poor globular clusters like M92 (Lee, Demarque, & Zinn 1994). Other hypotheses have been offered to explain the second-parameter phenomenon (Renzini 1978), and an increasing body of evidence suggests that age may be no more than a minor contributor to horizontal-branch morphology (Stetson, Vandenberg, & Bolte 1996). However, the debate is by no means settled, and the reader is referred to Lee et al. (1994) and Chaboyer, Demarque, & Sarajedini (1996) for arguments in support of the age hypothesis.

The best ground-based CCD CMDs of the Draco dwarf spheroidal galaxy to date have been presented by Stetson,

¹ Based on observations with the NASA/ESA *Hubble Space Telescope*, obtained at the Space Telescope Science Institute, which is operated by the Association of Universities for Research in Astronomy, Inc., under NASA contract NAS 5-26555.

² Department of Astronomy, Mail Stop 105-24, California Institute of Technology, Pasadena, CA 91125.

³ Mount Stromlo and Siding Spring Observatories, Institute of Advanced Studies, Australian National University, Private Bag, Weston Creek, ACT 2611, Australia.

⁴ Department of Astronomy, New Mexico State University, Box 30001/Department 4500, Las Cruces, NM 88003-8001.

⁵ Department of Astronomy, University of Michigan, 830 Dennison Building, 500 Church Street, Ann Arbor, MI 48109-1090.

⁶ Hubble Fellow.

⁷ Department of Atmospheric, Oceanic, and Space Sciences, Space Research Building, University of Michigan, Ann Arbor, MI 48109.

⁸ Astrophysics Division, Space Sciences Department, Space Telescope Science Institute, 3700 San Martin Drive, Baltimore, MD 21218.

⁹ Jet Propulsion Laboratory, California Institute of Technology, 4800 Oak Grove Drive, Pasadena, CA 91109-8099.

¹⁰ Department of Astronomy, University of Wisconsin at Madison, 475 North Charter Street, Madison, WI 53706.

¹¹ Department of Physics and Astronomy, Johns Hopkins University, 3400 North Charles Street, Baltimore, MD 21218.

¹² Department of Physics and Astronomy, Arizona State University, P.O. Box 871504, Tempe, AZ 85287.

¹³ Division of Geological and Planetary Sciences, Mail Stop 170-25, California Institute of Technology, 1200 East California Boulevard, Pasadena, CA 91125.

VandenBerg, & McClure (1985) and Carney & Seitzer (1986, hereafter CS86). Like the Ursa Minor dwarf spheroidal galaxy (the second-faintest known dwarf spheroidal galaxy), Draco appears to be as old as the oldest globular clusters, though CS86 and others discuss evidence from blue stragglers for an intermediate-age population as well.

The superb resolution afforded by the Wide Field Planetary Camera 2 (WFPC2) on the *Hubble Space Telescope* (*HST*) permits a remarkable improvement in our ability to study the stellar content of the Draco dwarf spheroidal galaxy, as well as other galaxies in the Local Group. Here we describe the first results of an *HST* program to investigate the stellar population of this galaxy.

2. OBSERVATIONS AND PHOTOMETRY

The images we presently discuss were taken on 1995 June 9 with WFPC2. The region selected for WFPC2 imaging is

shown overlaid on the Digital Sky Survey in Figure 1, and is roughly centered on field 1 of CS86. One 200 s and two 1000 s exposures were taken in F606W ($\sim V$), while the F814W ($\sim I$) images are composed of 200, 1100, and 1300 s integration times. F606W was chosen over F555W to obtain a somewhat higher signal-to-noise ratio. In the process of cosmic-ray removal, the exposures in each filter were combined into single, composite images from which subsequent photometry was derived. A mosaic of the coded WFPC2 frames in F814W is shown in Figure 2.

Photometry on the three Wide Field (WF) detectors ($0''.0996 \text{ pixel}^{-1}$) was carried out using a combination of aperture photometry and ALLFRAME point-spread function (PSF) fitting photometry (Stetson 1994). ALLFRAME is the latest development in the DAOPHOT series of photometry packages and differs from its predecessors primarily in its ability to use information from many individual

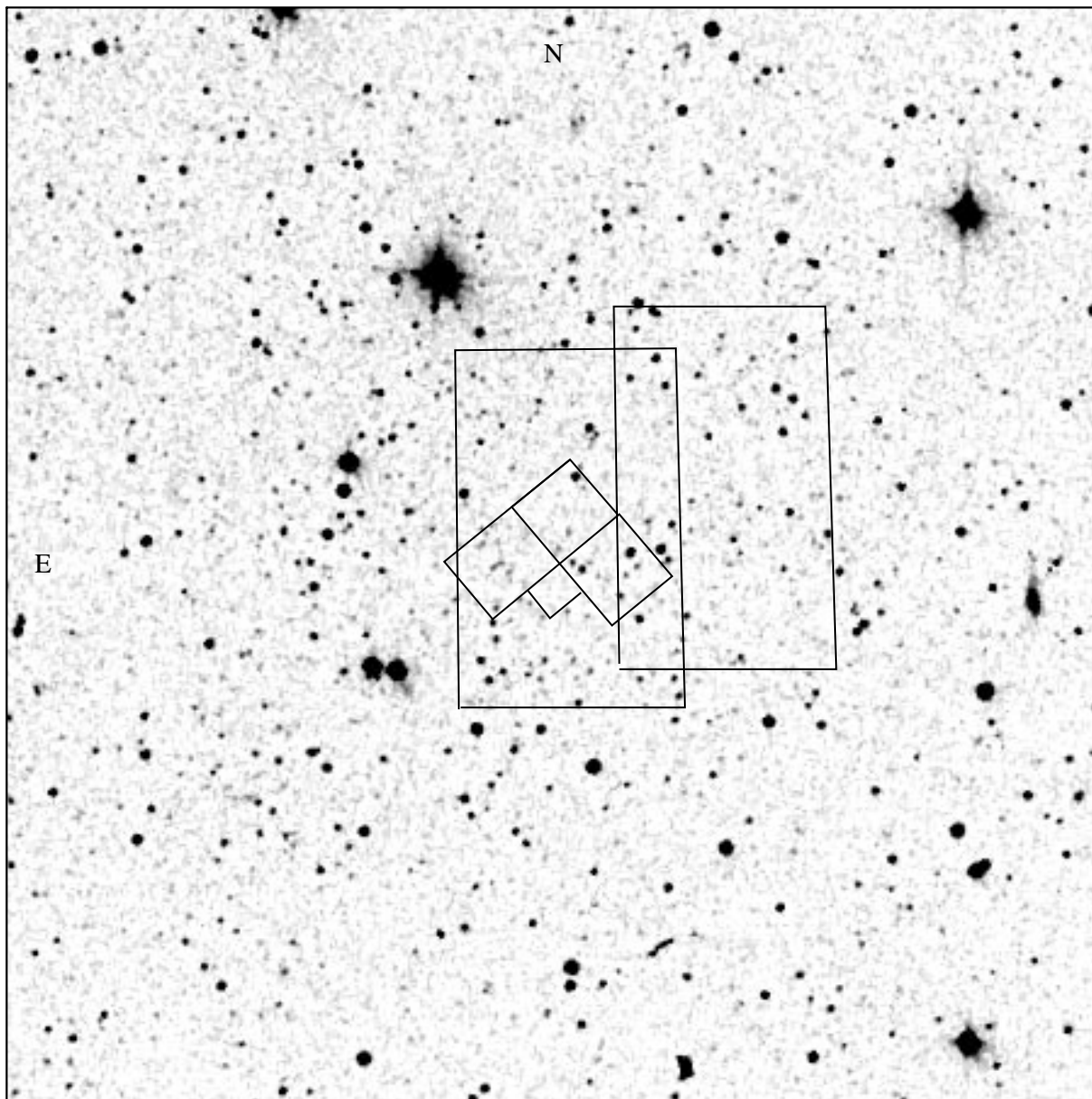


FIG. 1.—Digitized Sky Survey image of the field containing the Draco dwarf spheroidal galaxy. The outlines indicate the *HST* WFPC2 field and fields 1–2 of Carney & Seitzer (1986). The entire field shown subtends $15'$ on a side.

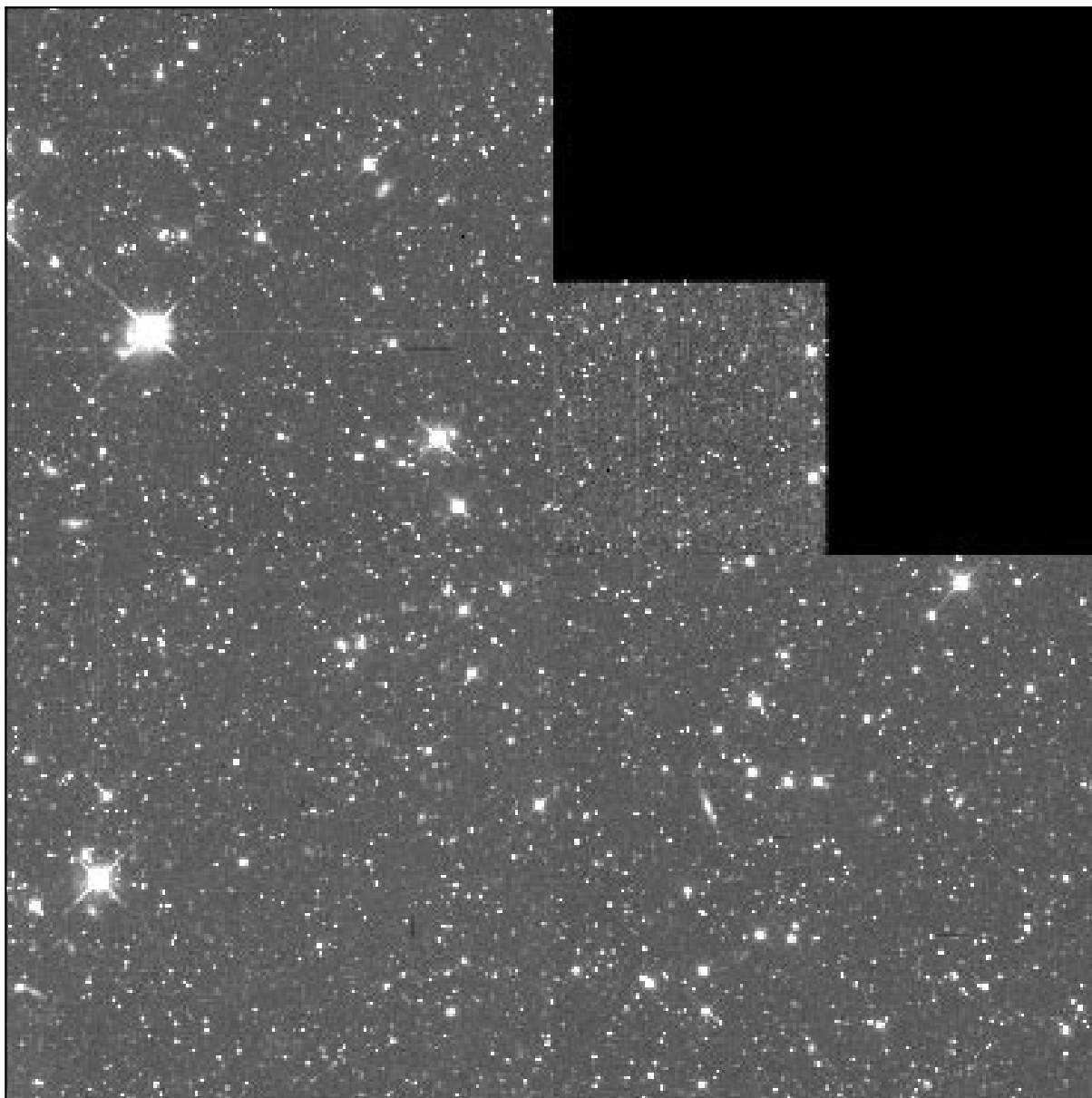


FIG. 2.—Mosaic of the co-added F814W frames

frames simultaneously to better constrain the final fitted magnitudes. ALLFRAME is applied to the data *after* object detection and aperture photometry is carried out using DAOPHOT II (Stetson 1987).

To push the star detection limit to as faint a level as possible, we co-added all images taken through the *same* filter. Co-adding the F606W and F814W images prior to object detection might in principle seem to offer an even fainter detection limit, but doing so would have significantly complicated subsequent completeness determinations. Two DAOPHOT detection passes were carried out, separated by photometry and subtraction of all stars found in the first pass. Faint stars hidden within the PSF skirts of brighter companions were thereby revealed and subsequently added to the list of detected stars to be measured. PSFs for each detector and each filter were constructed within DAOPHOT using the ~ 20 brightest and most isolated point sources in each frame. ALLFRAME was then applied to the F606W and F814W images simultaneously. A total of

4425 stars were ultimately detected and measured in the three WF frames.

Because of the degree of undersampling and relatively poor PSF representation in the WF chips, PSF fitting of brighter stars is subject to greater uncertainties in the absence of crowding than is pure synthetic aperture photometry. However, crowding and poor signal-to-noise ratio become ever-increasing problems as one considers fainter and fainter stars, and the ALLFRAME-derived magnitudes yield a tighter main sequence than is obtainable using aperture photometry. In order to retain the small uncertainties associated with aperture photometry of bright, uncrowded giants and to simultaneously extend the main sequence as far as possible, the CMD was constructed using both aperture and PSF-fitted magnitudes. The aperture magnitudes were used whenever the predicted total light within an aperture of radius 2 pixels from all other resolved stars (based on the known characteristics of the WFPC2 PSF) within $2''$ was less than 1% of the light from the star centered in the

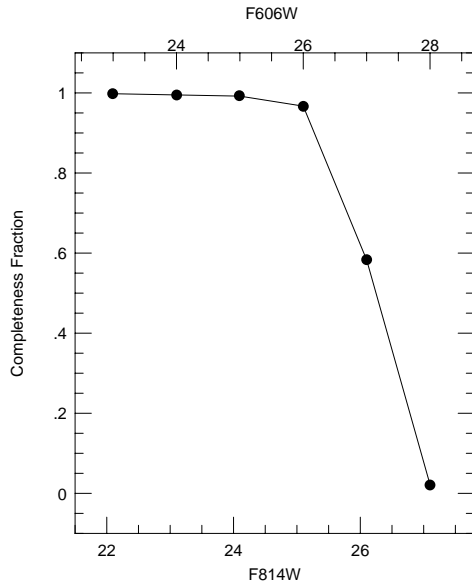


FIG. 3.—Completeness fraction as a function of F606W and F814W magnitude. Completeness tests were made using artificial stars of color $F606W - F814W \approx 0.9$ mag.

aperture. Corrections to a $0''.5$ aperture were made in each case, and the synthetic zero points of Holtzman et al. (1995) were used to compute WFPC2 system magnitudes.

Completeness tests were carried out by adding ≈ 100 stars at a time to each of the F606W and F814W images. Stars were added in integer F814W steps, and with $F606W - F814W \approx 0.9$ mag. The frames were then processed using DAOPHOT II and ALLFRAME in a manner identical to that applied to the original data. The results of these tests are shown in Figure 3, which shows that the 50% completeness level occurs at $F814W \approx 26.2$. The faintest stars that we can reliably measure have masses of $\sim 0.6 M_{\odot}$. The tests also show that the photometric uncertainties are ± 0.06 mag rms at $F814W = 23$, and ± 0.11 mag rms at $F814W = 25$.

3. DISCUSSION

3.1. Morphology of the Color-Magnitude Diagram

The F814W versus $F606W - F814W$ CMD, constructed using both aperture photometry for uncrowded stars (269) and ALLFRAME fits for crowded stars (4156), is shown in Figure 4. An electronic version of the photometry table is available upon request from C. J. G.

The morphology in Figure 4 above the turnoff is very similar to that found by Stetson et al. (1985) and CS86. As a result of the superior resolution afforded by the *HST* data, we are able to extend the main sequence 2 mag fainter than these ground-based studies. The turnoff region is well resolved and reveals that the bluest main-sequence stars have $F606W - F814W = 0.36$. There are, evidently, fewer blue stragglers than in the CMD of CS86, consistent with a ratio of ~ 5 in field of view. Unlike CS86, we see no evidence for distinct multiple turnoffs; most of the stars within the WFPC2 field of view appear to be approximately coeval. We caution, however, that while our photometry may be more accurate, we have sampled only one-fifth as many stars in the turnoff region as have CS86, and it may be premature to rule out the multiple turnoffs in Draco. Addi-

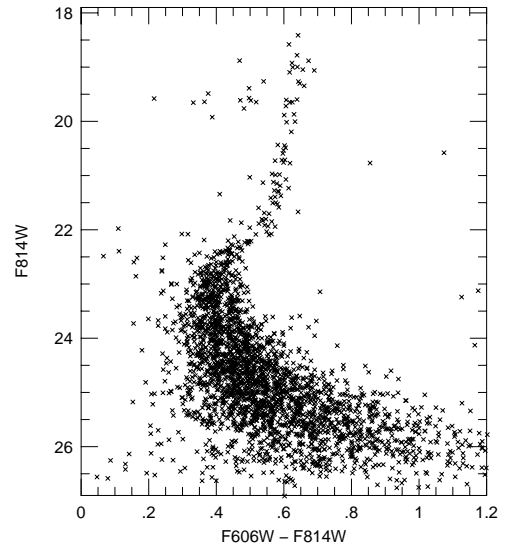


FIG. 4.—*HST* CMD of the Draco dwarf spheroidal galaxy. Most of the stars on the giant branch were measured using aperture photometry, while the majority of stars below the turnoff were measured by fitting PSFs.

tional WFPC2 fields of Draco will be required before we can seriously address this issue.

3.2. Age

In Figure 5, we compare the Draco CMD with fiducial sequences for the Galactic globular clusters M68 (Walker 1994) and M92 (Heasley & Janes 1997), which have $[Fe/H] = -2.09$ and -2.24 dex, respectively (Djorgovski 1993). The Draco magnitudes have been dereddened assuming $E(B - V) = 0.03$ (Stetson 1979a), using the absorptions tabulated by Holtzman et al. (1995) for stars of K5 spectral type. The globular cluster sequences were dereddened and translated using the color excesses and distances tabulated by Peterson (1993). A mean abundance for giants in Draco has

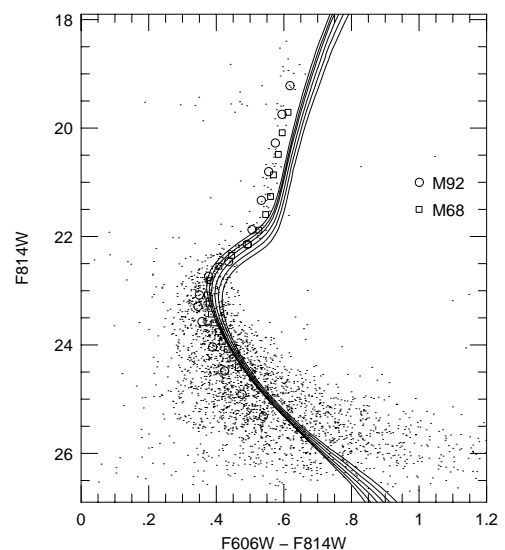


FIG. 5.—CMD of the Draco dwarf spheroidal galaxy compared with fiducial sequences for the metal-poor globular clusters M68 and M92. Superposed are Worthey (1994) models for an age of 16 Gyr, spanning metallicities of $[Fe/H] = -2.2$ (left) to $[Fe/H] = -1.2$ (right). The globular cluster sequences have been transformed from V and I to F606W and F814W using the transformation coefficients given by Holtzman et al. (1995).

been spectroscopically measured to be $[Fe/H] \approx -1.9$ dex (Lehnert et al. 1992). Adopting a mean horizontal-branch magnitude $\langle m_V \rangle = 20.07 \pm 0.03$ (Stetson 1979a), $E(B-V) = 0.03$ (Stetson 1979b), and $M_V = 0.15[Fe/H] + 0.82$ (Carney, Storm, & Jones 1992), we use $(m-M)_0 = 19.48$. The isochrones shown in Figure 5 are from Vandenberg & Bell (1985), with colors from the $V-K$ versus T_{eff} relations for dwarfs from Johnson (1966), and for giants from Ridgway et al. (1980). $V-K$ colors have been transformed to $V-I$ empirically and in the correct metallicity regime via the preliminary multimetallicity color-color diagrams of Worthey & Fisher (1996), and $V-I$ have in turn been converted to $F606W - F814W$ using the transformation equations in Holtzman et al. (1995).

A sequence of normal points representing the color-magnitude sequence was generated by defining an inclusion envelope around the main sequence and the subgiant and giant branches and computing mean magnitudes and colors in 0.4 mag-wide bands. Because of the scarcity of giant-branch stars and the associated large uncertainties in their mean colors, the locus of the giant branch above $F814W = 20.5$ was estimated by eye. This sequence, resampled using spline fits, was then compared using a maximum likelihood technique with isochrones ranging in age from 12 to 18 Gyr, and with $[Fe/H]$ ranging from -1.2 to -2.2 . The normal points were uniformly weighted, and the best-fitting isochrone had an age of 16 Gyr and $[Fe/H] = -2.2$. Given the weighting of the data, a formal χ^2 estimate of the uncertainty was not straightforward, and the fitting uncertainty was instead estimated by generating 100 realizations of the sequence of normal points (using Gaussian deviations based on the dispersion in the mean colors in each magnitude bin) and comparing them with each of the isochrones. This yielded an age uncertainty, based purely on random and fitting errors, of 0.5 Gyr.

Shown in Figure 5 are isochrones corresponding to an age of 16 Gyr and $[Fe/H]$ ranging from -1.2 to -2.2 dex. An age of 16 Gyr is not atypical of ages found for several metal-poor Galactic globular clusters using this set of isochrones. However, despite the small uncertainty due to random effects, it is apparent from Figure 5 that there are clear, systematic differences between the isochrones and the data. Whereas the fiducial sequences of M68 and M92 agree reasonably well with the color-magnitude distribution of Draco stars, the isochrones generally appear too red, particularly along the giant branch. This is undoubtedly due in large part to the roundabout technique used above to transform values of T_{eff} to $F606W - F814W$ colors. Given the numerous calibrations involved and the systematic discrepancies that can arise, it is clearly dangerous to place much faith in the age we derive using this method.

A calibration-independent method for measuring relative ages¹⁴ has been described by Vandenberg, Bolte, & Stetson (1990). This involves measuring the difference in color between the turnoff and the giant branch, which is relatively insensitive to metallicity but is a monotonic function of age. In Figure 6, we show the fiducial sequence for Draco (generated as described above) compared with similar sequences for the Galactic globular clusters M68 and M92.

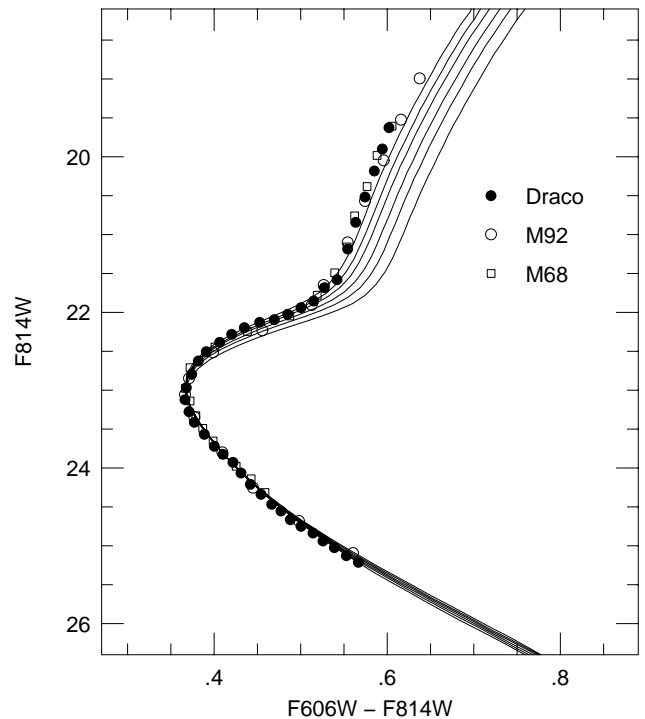


FIG. 6.—Fiducial sequence for Draco compared with similar sequences for the Galactic globular clusters M68 and M92, using the relative age measuring technique described by Vandenberg et al. (1990). The M68 and M92 sequences, measured in V and I , have been transformed to $F606W$ and $F814W$ using the synthetic transformation discussed in the text. The cluster sequences and the Worthey (1994) models (having $[Fe/H] = -2.0$ and ages ranging from 13 Gyr [right] to 18 Gyr [left]) have been shifted horizontally to match the Draco sequence at the bluest point of the turnoff region, and vertically to agree with one another at a point 0.05 mag redward of the turnoff on the main sequence.

Also shown are isochrones having $[Fe/H] = -2.0$ and ages ranging from 13 to 18 Gyr. The globular cluster sequences and the isochrones have been shifted horizontally to match the Draco sequence at the bluest point of the turnoff region, and vertically to agree with one another at a point 0.05 mag redward of the turnoff on the main sequence. The Draco sequence evidently agrees very well with the globular cluster sequences, though there are small differences in the shape of the turnoff and the slope of the giant branch.

The relative ages between sequences are best measured via this technique by comparing the colors of the giant branch, where the color separation is largely independent of magnitude. Looking at the isochrone spacing, it is evident that the color difference between giant branches is not uniform, but depends on absolute age. If we calibrate age differences using the oldest (leftmost) two isochrones, then the mean color difference measured in the region $20 < F814W < 21$ (below the horizontal branch and in a region where the giant branch is relatively well sampled) yields a relative age difference between Draco and either of the globular clusters of considerably less than 1 Gyr. Note that using increasingly younger isochrones to establish the color difference-age calibration would reduce the inferred age differences even more.

Given the photometric scatter apparent on the main sequence, the presence of blue stragglers or large numbers of binary stars could conceivably affect the determination of the mean colors of the turnoff and the main sequence. To

¹⁴ We emphasize that our conclusions refer to *relative* ages. If RR Lyrae stars are as luminous as claimed by Reid (1997) and Alcock et al. (1997) ($M_V = 0.20$), then the *absolute* ages of the globular clusters (and Draco) are reduced by ~ 3 Gyr.

estimate our sensitivity to these effects, we have recomputed the Draco normal points using an inclusion envelope alternately more exclusive of stars on the blue side of the turnoff and on the red side of the main sequence. In the latter case, we have excluded approximately 3 times as many outliers to the red of the main sequence as to the blue. Using these computed normal sequences (in addition to a number of hand-sketched realizations), and bringing all other sequences into alignment as before, we estimate our measurement uncertainty to be ± 1 Gyr. The distribution of relative ages measured in this way is slightly asymmetric, in the sense that an older Draco is preferred over a younger.

Additional uncertainty arises from possible errors in the color terms used to transform between photometric systems. Two such color terms are used here: the term used to transform the ground-based data into $V-I$, and that used to transform $V-I$ into $F606W-F814W$. The close similarity in age we infer for M68 and M92 agrees with the results of Vandenberg et al. (1990) based on independent BV data sets and suggests that errors in the ground-based color terms are likely to be small. Errors in the transformation from $V-I$ to $F606W-F814W$ arise from inaccuracies in the fitting formula used on the synthetic photometry results and from the error made by applying a transformation based on stars of solar metallicity to a metal-poor population. We estimate that fitting errors would introduce an error of order 0.02 mag in the difference in color between the turnoff and the giant branch. This translates to an age uncertainty of about 2.3 Gyr.

Applying transformation coefficients based on solar-metallicity stars to the more metal-poor stars of M68 and M92 has the effect of making the globular cluster giant branches in Figure 6 appear somewhat bluer relative to Draco than they should. Using Kurucz model atmospheres, we find that stars at the turnoff and on the giant branch are fainter in $F606W$ by 0.014 and 0.024 mag, respectively, than what we compute using the Holtzman et al. (1995) coefficients. The $F814W$ transformation for these stars is much less sensitive to metallicity, and we estimate that the differences in $F606W-F814W$ color between the turnoffs and the giant branches of M68 and M92 should be about 0.014 mag larger than shown. Correcting our measured result accordingly and combining the two major sources of error above, we conclude that Draco is 1.6 ± 2.5 Gyr older than either M68 or M92.

Given the very different HB morphologies of Draco and the two globular clusters, what can we say about the second-parameter problem? In Figure 7 we partially reproduce the $[\text{Fe}/\text{H}]$ versus HB morphology diagram of Lee et al. (1994). We have determined the morphological type quantity $(B-R)/(B+V+R)$ for Draco using the CMDs of both Stetson (1979a) and CS86. Counting stars on the blue and red sides of the instability strip, as well as likely RR Lyrae variables, we find $(B-R)/(B+V+R) = -0.77$ and -0.70 for the two data sets, respectively. We plot the mean of these two values in Figure 7 along with similar quantities tabulated by Lee et al. (1994) for M68 and M92. For both uniform mass-loss models and models in which the mass-loss rate increases with age (Reimers 1977), the Draco point appears to fall about 2 Gyr below the isochrone that best matches M68 and M92. As this is only 1.4 times greater than our estimated age uncertainty, we cannot completely rule out consistency between Draco and an age-dependent horizontal-branch morphology of the type modeled by Lee

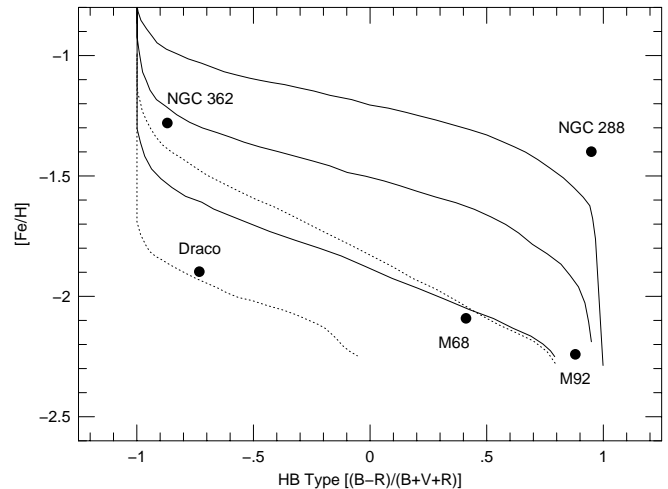


Fig. 7.—Partial reproduction of Lee et al.'s (1994) Fig. 9a, which they use to demonstrate a relation between horizontal-branch morphology and age. The solid lines correspond to models that assume uniform stellar mass loss and are separated by 2 Gyr. The dashed lines are also separated by 2 Gyr and assume a mass-loss rate that increases with age. The plotted values for various globular clusters are taken from the compilation of Lee et al. (1994), and the HB type for Draco was computed using the CMDs of Stetson (1979a) and Carney & Seitzer (1986).

et al. (1994). WFPC2 photometry of old globular clusters, sufficient to reduce the relative age uncertainty to ~ 0.5 Gyr, will be required before we can put firmer constraints on the models.

4. STAR FORMATION HISTORY

Zinn (1978) and Lehnert et al. (1992) have demonstrated an abundance spread of approximately 1 dex in Draco. Aside from this chemical inhomogeneity, how well does the Draco dwarf spheroidal galaxy fit the *simple stellar population* paradigm of Renzini & Buzzoni (1986)? We have seen that the turnoff CMD morphology of Draco is very similar to that of M92; globular clusters are the prototypical simple stellar populations, coeval systems of initially homogeneous composition. Clearly, Draco is predominantly a simple stellar population originating as early as anything in the Galaxy.

Close examination of the CMD shows a significant population of blue stragglers (see also CS86). Such stars are often observed in simple stellar populations, including both ancient globular and younger open star clusters, but they can also result from an *extended* star formation history. We can count them in color profiles (Fig. 8) formed out of half-magnitude strips from the turnoff region. The surface density of foreground stars in this region of the CMD (specifically, a region 0.3 mag wide in color and 2 mag high in $F606W$) is predicted by the Galactic model of Bahcall & Soneira (1980) to be 17 per square degree. Thus, there is only a 2% probability of finding a single foreground star among the ~ 17 stars we identify as blue stragglers (roughly speaking, those stars with $F814W < 23$ and $F606W-F814W < 0.3$). There are between 60 and 70 stars in the same region ($V < 23$ and $B-V < 0.3$) of the CMD of CS86. Given that the area surveyed by CS86 is about 5 times that of the area covered by our WFPC2 field, a ratio of 3.8 ± 1 in the number of blue stragglers indicates reasonable agreement.

Simulations of the turnoff region using the Yale isochrones (Green, Demarque, & King 1984) require 6% of the

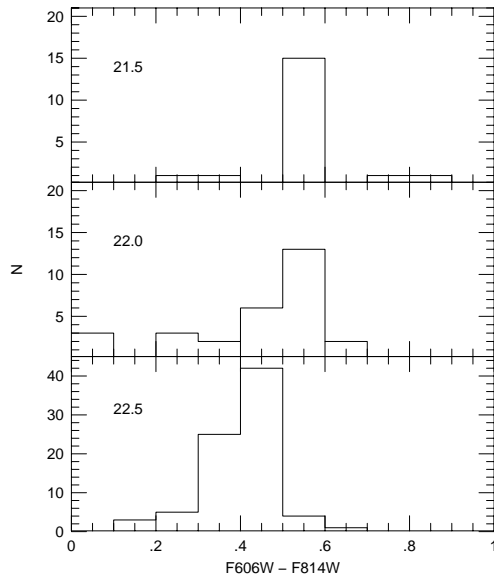


FIG. 8.—Color profiles generated by counting stars lying within half-magnitude-wide F814W bins. We attribute the excess number of blue stars over a putative Gaussian color distribution to the presence of ~ 17 blue stragglers.

mass to be contained in a second population, half the age of the primary population, in order to fully account for the blue stragglers in Figure 4. We note that 6% is an upper limit on the size of a second younger component of Draco, since blue stragglers can be an intrinsic part of a simple stellar population.

A putative extended star formation history strengthens the link between Draco and more fully developed examples of this phenomenon, such as Carina (Smecker-Hane et al. 1994, 1996). The difference between Draco and Carina and galaxies such as LGS 3 (Mould 1997) that are still forming stars today (at 10% of the original rate in the latter case) is then one of degree. Draco simply had a shorter tail to its initial burst of star formation. There is considerable evidence that wind-induced mass loss cannot account for the stellar populations seen in several Local Group dwarfs, and that stripping or capture of gas must have occurred (see Gallagher & Wyse 1994 for a review). Draco is currently among the nearest of the dwarf galaxies, and if its orbit is largely contained within its present distance, the probability of capturing significant amounts of rejuvenating circumgalactic gas may be substantially smaller than for dwarfs in the outskirts of the Local Group. Alternatively, a high ultraviolet flux from the precursors to the Galaxy and M31 may have removed substantially more gas from the nearby dwarfs (van den Bergh 1994).

None of these remarks bear at all on the better known curious phenomenon of Draco's red horizontal branch. The discovery that Draco is as old or older than M92 requires us to focus on the problem of understanding Draco's red horizontal branch. Higher signal-to-noise ratio (and preferably F555W – F814W) photometry performed differentially with respect to $[\text{Fe}/\text{H}] = -2$ clusters have the potential to sharpen our conclusions further. If the relative age uncertainty could be reduced to 0.5 Gyr, one would have to turn to parameters such as cluster density (e.g., Fusi Pecci et al. 1996) as the second parameter in the globular cluster system. The age spread of the halo, which is the defining

feature of the Searle & Zinn (1978) galaxy formation scenario (as opposed to that of Eggen, Lynden-Bell, & Sandage 1962) would then need to be defined by the ages of the low-density element of the halo, namely, Draco, its sibling dwarf spheroidals, and the Galactic bulge.

4.1. Initial Mass Function

Figure 9 shows the differential luminosity function (LF) for the stars in our sample. Also shown is an LF computed from Walker's (1994) photometry of M68. No completeness corrections have been applied to the M68 data, and the counts have been arbitrarily normalized to our data at F814W = 23. Note that the number of measured stars in the M68 sample is about 6 times larger than in the Draco sample. The Draco LF appears to be somewhat steeper on the giant branch, and somewhat shallower below the turnoff. Uncertainties introduced by differences in noise characteristics, resolution, and detection efficiency make it difficult to draw firm conclusions, but over the (admittedly narrow) mass range considered here, there does not appear to be an obvious bias toward lower mass stars, which might be held to account for the very high estimates of Draco's mass-to-light ratio. Based on the present data set, all we can say is that if the bulk of the matter is in the form of stars, such stars must have masses less than $0.6 M_{\odot}$.

The observed LF can be used to place limits on the IMF in Draco. The current observations are of stars with masses between 0.6 and $0.9 M_{\odot}$. We parameterize the IMF in this mass range by a simple power law, with $dN/dM \propto M^{\alpha}$. Even stars of this low mass evolve significantly over a Hubble time, so the inferred IMF slope depends on the age of the stellar population in Draco.

We construct model LFs using a variety of IMFs and compare each model distribution with the one observed to see if it is plausible that they are drawn from the same parent population. The construction of model LFs allows us to incorporate photometric errors (both random and systematic) and incompleteness into the analysis; the

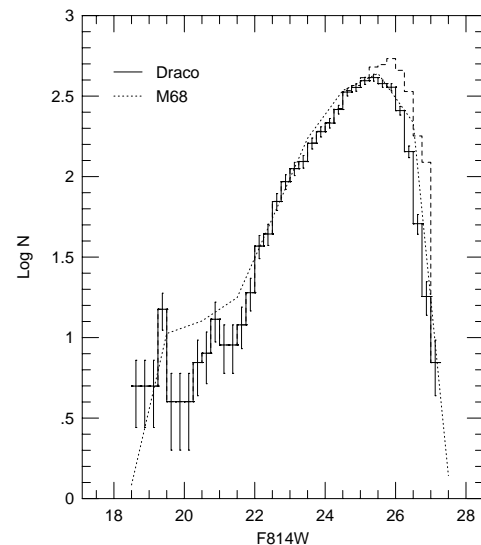


FIG. 9.—Differential LF of the stars in Draco. The error bars reflect Poisson errors only, and the dashed histogram shows the effect of dividing by the completeness function. Note that no account has been taken of bin-jumping due to photometric errors. The dotted line shows a luminosity function derived from Walker's (1994) M68 photometry *without* having applied completeness corrections.

incompleteness and errors that we apply to the model LFs are those determined from our artificial-star experiments. We can also include the effect of a binary star contribution if we make an assumption about the frequency and distribution of the relative masses of stars in binary pairs. For Draco, we assume a metallicity of $[Fe/H] = -2$ and a distance and extinction as quoted above, and use VandenBerg (1983) isochrones (from which Worthey's models are derived for low-mass stars) along with Kurucz model atmospheres to convert from masses to assumed luminosities.

We define as unacceptable IMF slopes for which the model LF and the observed LF are inconsistent with each other at the 95% confidence level as determined by a Kolmogorov-Smirnov test. With this definition, we constrain the IMF slope to fall within the range

$$\alpha > -1.00 \text{ for an assumed age of 18 Gyr,}$$

$$-1.52 > \alpha > -1.98 \text{ for an assumed age of 15 Gyr,}$$

$$-2.14 > \alpha > -2.30 \text{ for an age of 12 Gyr, and}$$

$$-2.48 > \alpha > -2.56 \text{ for an age of 10 Gyr}$$

when we fit the F606W LF over the range $1 < M_{F606W} < 7.25$ with stellar models of a single metallicity, $[Fe/H] = -2$. The dependence on age is easy to understand: as a population evolves, the LF around the turnoff steepens, leading to a flatter inferred IMF for an older population. These results were derived assuming a binary fraction of 0.5 with uncorrelated masses of the binary stars; with no binaries, we obtain slopes that are slightly shallower. Similarly, small variations on the above allowed ranges are derived with different assumptions about the metallicity, distance, and/or a different adopted magnitude range over which the comparison with the observed LF is made.

If we fit the F814W LF, we infer a range of possible IMF slopes that are slightly steeper than those inferred from the F606W LF. In the case of no binaries, the inferred slope range overlaps between the two bandpasses; for a binary

fraction of 0.5, all of the acceptable IMF slopes for F814W are steeper than those allowed by the F606W LF.

For comparison, the IMF in this mass range in the solar neighborhood is proportional to $M^{-2.2}$ (Kroupa, Tout, & Gilmore 1993). The allowed slopes for Draco are remarkably similar to this value.

5. CONCLUSIONS

Based on photometry of WFPC2 images of the Draco dwarf spheroidal, we conclude the following:

1. Draco is predominantly an old system, being 1.6 ± 2.5 Gyr older than either M68 or M92.

2. We see no evidence for multiple turnoffs that would be indicative of episodic star formation.

3. The presence of significant numbers of blue stragglers *may* indicate an extended period of star formation, though the numbers of younger stars is less than 6% of the first generation.

4. The luminosity function appears in all respects nearly identical to that of the old globular cluster M68.

5. The slope of the IMF appears to be very similar to that of the IMF determined for the solar neighborhood.

Future work should be aimed at refining the relative ages of Draco and blue horizontal branch clusters such as M92. Obtaining both higher signal-to-noise ratio data and WFPC2 color-magnitude diagrams of metal-poor globular clusters should allow us to reduce the relative age uncertainty to ≈ 0.5 Gyr. Such data would considerably strengthen constraints on the process and mechanisms that led to the formation of our Galaxy.

We are grateful to Gary da Costa for a critical reading of an earlier version of this manuscript. This research was conducted by the WFPC2 Investigation Definition Team, supported in part by NASA grant NAS 7-1260.

REFERENCES

- Aaronson, M. 1983, *ApJ*, 266, L11
 Alcock, C., et al. 1997, *ApJ*, in press
 Armandroff, T. E., Olszewski, E. W., & Pryor, C. 1995, *AJ*, 110, 2131
 Baade, W., & Swope, H. 1961, *AJ*, 66, 300
 Bahcall, J. N., & Soneira, R. M. 1980, *ApJS*, 44, 73
 Carney, B. W., & Seitzer, P. 1986, *AJ*, 92, 23 (CS86)
 Carney, B. W., Storm, J., & Jones, R. V. 1992, *ApJ*, 386, 663
 Chaboyer, B., Demarque, P., & Sarajedini, A. 1996, *ApJ*, 459, 558
 Djorgovski, S. 1993, in *ASP Conf. Ser. 50, Structure and Dynamics of Globular Clusters*, ed. S. Djorgovski & G. Meylan (San Francisco: ASP), 373
 Eggen, O. J., Lynden-Bell, D., & Sandage, A. R. 1962, *ApJ*, 136, 748
 Fusi Pecci, F., Bellazzini, M., Ferraro, F. R., Buonanno, R., & Corsi, C. E. 1996, in *ASP Conf. Ser. 92, Formation of the Galactic Halo—Inside and Out*, ed. H. Morrison & A. Sarajedini (San Francisco: ASP), 221
 Gallagher, J. S., III, & Wyse, R. F. G. 1994, *PASP*, 106, 1225
 Green, E. M., Demarque, P., & King, C. R. 1987, *The Revised Yale Isochrones and Luminosity Functions* (New Haven: Yale Univ. Obs.)
 Heasley, J., & Janes, K. 1997, in preparation
 Holtzman, J. A., Burrows, C. J., Casertano, S., Hester, J. J., Trauger, J. T., Watson, A. M., & Worthey, G. 1995, *PASP*, 107, 1065
 Johnson, H. L. 1966, *ARA&A*, 4, 193
 Koo, D. C., et al. 1994, *ApJ*, 469, 535
 Kroupa, P., Tout, C. A., & Gilmore, G. 1993, *MNRAS*, 262, 545
 Lee, Y. W., Demarque, P., & Zinn, R. 1994, *ApJ*, 423, 248
 Lehnert, M. D., Bell, R. A., Hesser, J. E., & Oke, J. B. 1992, *ApJ*, 395, 466
 Mould, J. R. 1997, *PASP*, 109, 125
 Peterson, C. J. 1993, in *ASP Conf. Ser. 50, Structure and Dynamics of Globular Clusters*, ed. S. Djorgovski & G. Meylan (San Francisco: ASP), 337
 Reid, I. N. 1997, *AJ*, in press
 Reimers, D. 1977, *A&A*, 57, 395
 Renzini, A. 1978, in *Advanced Stages of Stellar Evolution*, ed. A. Maeder (Geneva: Geneva Obs.)
 Renzini, A., & Buzzoni, A. 1986, in *Spectral Evolution of Galaxies*, ed. C. Chiosi (Dordrecht: Reidel), 195
 Ridgway, S. T., Joyce, R. R., White, N. M., & Wing, R. F. 1980, *ApJ*, 235, 126
 Searle, L., & Zinn, R. 1978, *ApJ*, 225, 357
 Smecker-Hane, T. A., Stetson, P. B., Hesser, J. E., & Lehnert, M. D. 1994, *AJ*, 108, 507
 Smecker-Hane, T. A., Stetson, P. B., Hesser, J. E., & VandenBerg, D. A. 1996, in *ASP Conf. Ser. 98, From Stars to Galaxies*, ed. C. Leitherer, U. Fritze-von Alvensleben, & J. Huchra (San Francisco: ASP), 328
 Stetson, P. 1979a, *AJ*, 84, 1149
 ———. 1979b, *AJ*, 84, 1167
 ———. 1987, *PASP*, 99, 191
 ———. 1994, *PASP*, 106, 250
 Stetson, P. B., VandenBerg, D. A., & Bolte, M. 1996, *PASP*, 108, 560
 Stetson, P. B., VandenBerg, D. A., & McClure, R. 1985, *PASP*, 97, 908
 VandenBerg, D. A. 1983, *ApJS*, 51, 29
 VandenBerg, D. A., & Bell, R. A. 1985, *ApJS*, 58, 561
 VandenBerg, D. A., Bolte, M., & Stetson, P. B. 1990, *AJ*, 100, 445
 van den Bergh, S. 1994, *ApJ*, 428, 617
 Walker, A. 1994, *AJ*, 108, 555
 Worthey, G. 1994, *ApJS*, 95, 107
 Worthey, G., & Fisher, B. 1996, *BAAS*, 189, No. 72.05
 Zinn, R. 1978, *ApJ*, 225, 790